Measurement of the Z-Boson p_T Distribution in $\bar{p}p$ Collisions at $\sqrt{s} = 1.8$ TeV

F. Abe,[9] D. Amidei,[4] G. Apollinari,[15] M. Atac,[4] P. Auchincloss,[14] A. R. Baden,[6] M. Bailey,[13] A. Bamberger,[4],[a] B. A. Barnett,[8] A. Barbaro-Galtieri,[10] V. E. Barnes,[13] T. Baumann,[6] F. Bedeschi,[12] S. Behrends,[2] S. Belforte,[12] G. Bellettini,[12] J. Bellinger,[20] J. Bensinger,[2] A. Beretvas,[4] J. P. Berge,[4] S. Bertolucci,[5] S. Bhadra,[7] M. Binkley,[4] R. Blair,[1] C. Blocker,[2] V. Bolognesi,[12] A. W. Booth,[4] C. Boswell,[8] G. Brandenburg,[6] D. Brown,[6] E. Buckley-Geer,[16] H. S. Budd,[14] A. Byon,[13] K. L. Byrum,[20] C. Campagnari,[3] M. Campbell,[3] R. Carey,[6] W. Carithers,[10] D. Carlsmith,[20] J. T. Carroll,[4] R. Cashmore,[4],[a] F. Cervelli,[12] K. Chadwick,[4] G. Chiarelli,[5] W. Chinowsky,[10] S. Cihangir,[4] A. G. Clark,[4] D. Connor,[11] M. Contreras,[2] J. Cooper,[4] M. Cordelli,[5] R. Cousins,[6],[a] D. Crane,[4] M. Curatolo,[5] C. Day,[4] S. Dell'Agnello,[12] M. Dell'Orso,[12] L. Demortier,[2] P. F. Derwent,[3] T. Devlin,[16] D. DiBitonto,[17] R. B. Drucker,[10] J. E. Elias,[4] R. Ely,[10] S. Eno,[3] S. Errede,[7] B. Esposito,[5] G. J. Feldman,[6] B. Flaugher,[4] G. W. Foster,[4] M. Franklin,[6] J. Freeman,[4] H. Frisch,[3] Y. Fukui,[9] Y. Funayama,[18] A. F. Garfinkel,[13] A. Gauthier,[7] S. Geer,[6] P. Giannetti,[12] N. Giokaris,[15] P. Giromini,[5] L. Gladney,[11] M. Gold,[10] K. Goulianos,[15] H. Grassmann,[12] C. Grosso-Pilcher,[3] C. Haber,[10] S. R. Hahn,[4] R. Handler,[20] K. Hara,[18] R. M. Harris,[10] J. Hauser,[3] C. Hawk,[16] T. Hessing,[17] R. Hollebeek,[11] L. Holloway,[7] P. Hu,[16] B. Hubbard,[10] B. T. Huffman,[13] R. Hughes,[11] P. Hurst,[5] J. Huth,[4] M. Incagli,[12] T. Ino,[18] H. Iso,[18] H. Jensen,[4] C. P. Jessop,[6] R. P. Johnson,[4] U. Joshi,[4] R. W. Kadel,[10] T. Kamon,[17] S. Kanda,[18] D. A. Kardelis,[7] I. Karliner,[7] E. Kearns,[6] L. Keeble,[17] R. Kephart,[4] P. Kesten,[2] R. M. Keup,[7] H. Keutelian,[7] S. Kim,[18] L. Kirsch,[2] K. Kondo,[18] J. Konigsberg,[6] S. E. Kuhlmann,[1] E. Kuns,[16] A. T. Laasanen,[13] J. I. Lamoureux,[20] S. Leone,[12] W. Li,[1] T. M. Liss,[7] N. Lockyer,[11] C. B. Luchini,[7] P. Maas,[4] M. Mangano,[12] J. P. Marriner,[4] R. Markeloff,[20] L. A. Markosky,[20] R. Mattingly,[2] P. McIntyre,[17] A. Menzione,[12] T. Meyer,[17] S. Mikamo,[9] M. Miller,[3] T. Mimashi,[18] S. Miscetti,[5] M. Mishina,[9] S. Miyashita,[18] Y. Morita,[18] S. Moulding,[2] J. Mueller,[16] A. Mukherjee,[4] L. F. Nakae,[2] I. Nakano,[18] C. Nelson,[4] C. Newman-Holmes,[4] J. S. T. Ng,[6] M. Ninomiya,[18] L. Nodulman,[1] S. Ogawa,[18] R. Paoletti,[12] A. Para,[4] E. Pare,[6] J. Patrick,[4] T. J. Phillips,[6] R. Plunkett,[4] L. Pondrom,[20] J. Proudfoot,[1] G. Punzi,[12] D. Quarrie,[4] K. Ragan,[11] G. Redlinger,[3] J. Rhoades,[20] M. Roach,[19] F. Rimondi,[4],[a] L. Ristori,[12] T. Rohaly,[11] A. Roodman,[3] W. K. Sakumoto,[14] A. Sansoni,[5] R. D. Sard,[7] A. Savoy-Navarro,[4] V. Scarpine,[7] P. Schlabach,[7] E. E. Schmidt,[4] M. H. Schub,[13] R. Schwitters,[6] A. Scribano,[12] S. Segler,[4] Y. Seiya,[18] M. Sekiguchi,[18] M. Shapiro,[10] N. M. Shaw,[13] M. Sheaff,[20] M. Shochet,[3] J. Siegrist,[10] P. Sinervo,[11] J. Skarha,[8] K. Sliwa,[19] D. A. Smith,[12] F. D. Snider,[8] L. Song,[11] R. St. Denis,[6] A. Stefanini,[12] G. Sullivan,[3] R. L. Swartz, Jr.,[7] M. Takano,[18] F. Tartarelli,[12] K. Takikawa,[18] S. Tarem,[2] D. Theriot,[4] M. Timko,[17] P. Tipton,[10] S. Tkaczyk,[4] A. Tollestrup,[4] J. Tonnison,[13] W. Trischuk,[6] Y. Tsay,[3] F. Ukegawa,[18] D. Underwood,[1] S. Vejcik, III,[8] R. Vidal,[4] R. G. Wagner,[1] R. L. Wagner,[4] N. Wainer,[4] J. Walsh,[11] T. Watts,[16] R. Webb,[17] C. Wendt,[20] W. C. Wester, III,[10] T. Westhusing,[12] S. N. White,[15] A. B. Wicklund,[1] H. H. Williams,[11] B. L. Winer,[10] A. Yagil,[4] A. Yamashita,[18] K. Yasuoka,[18] G. P. Yeh,[4] J. Yoh,[4] M. Yokoyama,[18] J. C. Yun,[4] and F. Zetti[12]

(CDF Collaboration)

[1]*Argonne National Laboratory, Argonne, Illinois 60439*
[2]*Brandeis University, Waltham, Massachusetts 02254*
[3]*University of Chicago, Chicago, Illinois 60637*
[4]*Fermi National Accelerator Laboratory, Batavia, Illinois 60510*
[5]*Laboratori Nazionali di Frascati, Istituto Nazionale di Fisica Nucleare, Frascati, Italy*
[6]*Harvard University, Cambridge, Massachusetts 02138*
[7]*University of Illinois, Urbana, Illinois 61801*
[8]*The Johns Hopkins University, Baltimore, Maryland 21218*
[9]*National Laboratory for High Energy Physics (KEK), Ibaraki, Japan*
[10]*Lawrence Berkeley Laboratory, Berkeley, California 94720*
[11]*University of Pennsylvania, Philadelphia, Pennsylvania 19104*
[12]*Istituto Nazionale di Fisica Nucleare, University and Scuola Normale Superiore of Pisa, I-56100 Pisa, Italy*

[13]*Purdue University, West Lafayette, Indiana 47907*
[14]*University of Rochester, Rochester, New York 14627*
[15]*Rockefeller University, New York, New York 10021*
[16]*Rutgers University, Piscataway, New Jersey 08854*
[17]*Texas A&M University, College Station, Texas 77843*
[18]*University of Tsukuba, Tsukuba, Ibaraki 305, Japan*
[19]*Tufts University, Medford, Massachusetts 02155*
[20]*University of Wisconsin, Madison, Wisconsin 53706*
(Received 1 August 1991)

We have measured the Z-boson production differential cross section as a function of transverse momentum using $Z \rightarrow ee$ and $Z \rightarrow \mu\mu$ decays in $\bar{p}p$ collisions at $\sqrt{s} = 1.8$ TeV with the Collider Detector at Fermilab. Comparison with standard-model predictions shows good agreement over the range $0 < p_T < 160$ GeV/c available from this data sample.

PACS numbers: 13.85.Qk

In the framework of quantum chromodynamics (QCD), the transverse momentum p_T of W and Z gauge bosons produced in $\bar{p}p$ collisions results from the production of quarks or gluons together with the gauge boson. Theoretical calculations of the inclusive W and Z production differential cross section as a function of p_T are now available at next-to-leading order for all p_T values at $\sqrt{s} = 1.8$ TeV [1]. A measurement of the boson p_T distribution provides a test of standard-model predictions. In this Letter, we report a measurement of the Z-boson differential cross section $d\sigma/dp_T$, using $Z \rightarrow ee$ and $Z \rightarrow \mu\mu$ decays in $\bar{p}p$ collisions at $\sqrt{s} = 1.8$ TeV with the Collider Detector at Fermilab (CDF). A measurement for W bosons is reported in Ref. [2]. Previous results on W and Z production at the CERN $\bar{p}p$ collider ($\sqrt{s} = 0.63$ TeV) have been reported in [3].

The CDF detector is described in detail elsewhere [4]. The components of the CDF relevant for this analysis are described briefly here. A time-projection chamber (VTPC) measures the event vertex and provides tracking information. A central tracking chamber (CTC) measures charged-particle momenta in a 1.4-T magnetic field. Calorimeters are organized into a projective tower geometry, with electromagnetic (EM) compartments followed by hadronic compartments. Scintillator calorimeters cover the central region, pseudorapidity $|\eta| < 1.1$. Proportional tube calorimeters cover the plug and forward regions, $1.1 < |\eta| < 2.4$ and $2.4 < |\eta| < 4.2$, respectively. In the central and plug EM calorimeters, proportional chambers imbedded near shower maximum measure shower position and shape. Drift chambers behind the central calorimeters in the region $|\eta| < 0.6$ are used for muon detection.

The muon momentum is determined in the CTC with a resolution of $\delta p_T/p_T = 0.0011 p_T$, with p_T in GeV/c. The electron energy is measured by the calorimeter. In the central region, the energy resolution is $(\sigma_E/E)^2 = [0.135/\sqrt{E_T\ (\mathrm{GeV})}]^2 + (0.02)^2$, where $E_T = E \sin\theta$ and θ is the polar angle with respect to the proton beam direction. In the plug and forward regions, the energy resolution is $\sigma_E/E = 0.28/\sqrt{E\ (\mathrm{GeV})} + 0.02$. The electron direction is given by the CTC track in the central region, and by the shower position in the plug and forward regions. The transverse momentum of the Z is the vector sum of the ee or $\mu\mu$ transverse momenta.

The $Z \rightarrow ee$ sample is selected from events satisfying the central electron trigger, which requires an EM cluster that has at least 12 GeV of E_T, a ratio of less than 0.125 for the hadronic to electromagnetic energy, and an associated CTC track with $p_T > 6$ GeV/c. We further require that there is at least one electron in the central region, and that (1) the electron E_T be > 20 GeV; (2) the ratio of energy to track momentum, E/p, be < 1.5; (3) the shower position match an extrapolated CTC track; (4) the shower shape and the energy leakage into the hadronic compartment be consistent with a test-beam electron shower; and (5) the electron be isolated (the energy accompanying the electron be consistent with energy deposition from the underlying event). In addition, we require a second isolated electron in the region $|\eta| < 4.2$ to have (1) $E_T > 10$ GeV; (2) if in the central region, $E/p < 2.0$; (3) if in the plug region, a VTPC track and a lateral shower profile consistent with a test-beam electron shower; and (4) small energy leakage into the hadronic compartment. Each electron is required to be inside a fiducial region away from calorimeter edges. The event vertex must be within 60 cm of the center of the detector. More details on the electron selection can be found elsewhere [5].

The $Z \rightarrow \mu\mu$ sample is selected from events satisfying the central muon trigger, which requires a track in the muon drift chamber, matched to a CTC track with $p_T > 9$ GeV/c. We further require that (1) the muon track match an extrapolated CTC track within 2 cm in the azimuthal direction; (2) the CTC track p_T be > 20 GeV/c; and (3) the energy deposited in the calorimeter tower associated with the track be consistent with that for a minimum ionizing particle. In addition, we only require the second muon candidate to have a CTC track with $p_T > 10$ GeV/c and $|\eta| < 1.0$, and to satisfy the minimum ionizing requirement. It is not restricted to be in the region covered by the muon drift chambers.

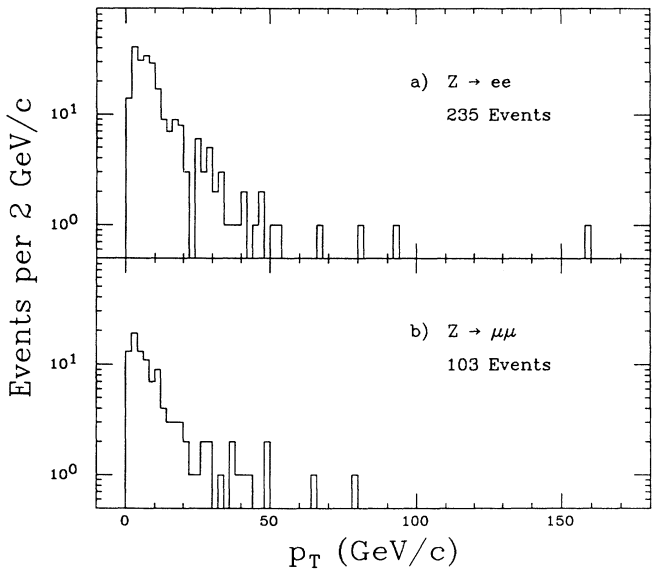

FIG. 1. The observed p_T distributions of (a) $Z \rightarrow ee$ and (b) $Z \rightarrow \mu\mu$ candidate events.

The lepton (e or μ) trigger and selection efficiencies are obtained from a sample of Z decay leptons. The muon trigger is $(93.7 \pm 3.1)\%$ efficient for our data sample. The muon selection efficiency is $(94.3 \pm 2.8)\%$ and $(92.7 \pm 2.1)\%$ for muons with and without a required track in the muon drift chamber, respectively. The electron trigger is $(97.2 \pm 0.4)\%$ efficient for our data sample. The electron selection efficiency is $(85.5 \pm 4.3)\%$ for the first central electron and $(92.0 \pm 4.1)\%$, $(92.4 \pm 4.4)\%$, and $(97.5 \pm 2.0)\%$ for the second central, plug, and forward electrons, respectively. The efficiencies are found to be independent of the Z p_T.

There are 235 $Z \rightarrow ee$ and 103 $Z \rightarrow \mu\mu$ candidate events with invariant mass between 75 and 105 GeV/c^2. The events outside the mass peak are consistent with the Drell-Yan continuum [6]. The backgrounds from QCD jet production are less than 1%. The $Z \rightarrow ee$ and $Z \rightarrow \mu\mu$ samples are combined in this measurement. The observed p_T distribution is shown in Fig. 1 [7].

We use the ISAJET [8] Monte Carlo program and a detector model to obtain corrections for p_T-dependent acceptance and resolution smearing effects. The corrections take into account the different acceptances and resolutions of the $Z \rightarrow \mu\mu$ and the $Z \rightarrow ee$ central-central, central-plug, and central-forward events. The detector model simulates fiducial regions, event vertex smearing, lepton momentum resolution, and lepton selection and trigger efficiencies. We use in the simulation a variety of parametrizations of the quark and gluon momentum distributions [9]; the Martin-Roberts-Stirling set B is used as the nominal set. The Monte Carlo p_T distribution is adjusted to fit the observed p_T spectrum. The systematic uncertainty due to assumptions made in the simulation is obtained by varying the model parameters. The acceptance is $(40 \pm 2)\%$ at $p_T = 1$ GeV/c and rises to $(56 \pm 7)\%$ at $p_T = 130$ GeV/c because the decay leptons of high-p_T Z's are boosted toward the central region, and we always require at least one central lepton.

The Z p_T, for the combined $Z \rightarrow ee$ and $Z \rightarrow \mu\mu$ data, is measured with an rms resolution of 1.5 GeV/c at $p_T = 2$ GeV/c and 4 GeV/c at $p_T = 130$ GeV/c. We correct for the effect of resolution smearing on the shape of the spectrum. A smearing matrix is derived from the Monte Carlo simulation. This matrix describes the probability that a given p_T is measured to have a different value due to resolution smearing. We use the inverse of this matrix to unfold the resolution smearing in the observed p_T spectrum [10].

TABLE I. Summary of results and uncertainties. The uncertainties are systematic and statistical combined. They are correlated among bins due to correction for resolution smearing. Also shown are elements of the correlation matrix $\rho_{ij} = \sigma_{ij}/(\sigma_{ii}\sigma_{jj})^{1/2}$, where σ_{ij} is the covariance matrix element for th ith and jth bins.

Δp_T (GeV/c)	Events observed	p_T (GeV/c)	$d\sigma/dp_T$ [pb/(GeV/c)]	Correlation coefficients $(i,i+1)$	$(i,i+2)$	$(i,i+3)$
0–2	27	1.0	391 ± 139	−0.45	0.07	−0.02
2–4	60	2.8	734 ± 214	−0.48	0.22	−0.10
4–7	66	5.6	251 ± 144	−0.50	0.23	−0.10
7–10	59	8.4	427 ± 110	−0.43	0.14	0.01
10–14	39	12.0	149 ± 55	−0.38	0.07	0.00
14–18	22	16.0	104 ± 38	−0.32	0.06	−0.01
18–23	17	20.3	61.5 ± 23.5	−0.29	0.08	0.00
23–28	12	25.3	44.6 ± 20.4	−0.35	0.04	0.01
28–33	10	30.4	38.7 ± 17.6	−0.18	0.02	0.00
33–45	14	38.4	21.5 ± 7.0	−0.15	0.02	0.00
45–65	6	54.0	4.7 ± 2.5	−0.17	0.02	···
65–90	4	76.3	2.8 ± 1.6	−0.10	···	···
90–180	2	126	0.3 ± 0.2	···	···	···

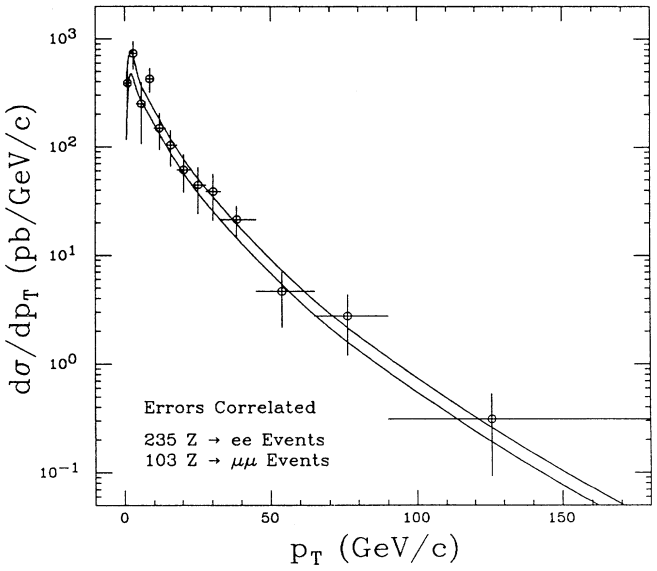

FIG. 2. The differential cross section for Z production. The next-to-leading-order QCD calculation is shown as a band; the width of the band indicates the theoretical uncertainty.

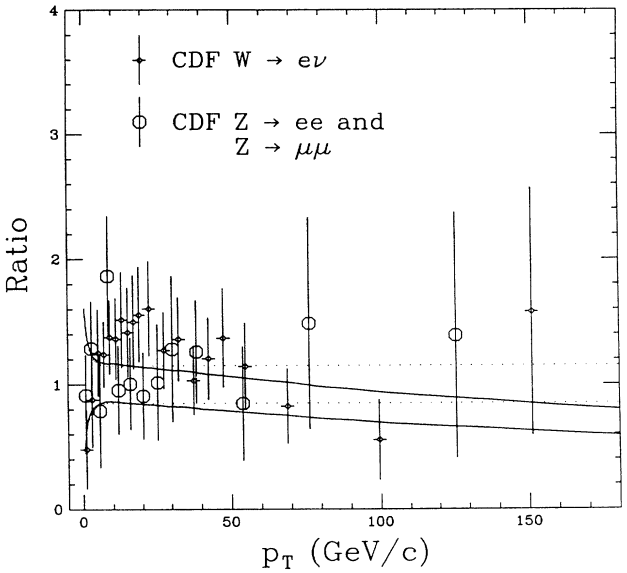

FIG. 3. The ratio of the W and Z p_T spectra to the nominal QCD prediction for the Z; the W's are normalized by the ratio of the measured W and Z total cross sections [5]. The QCD prediction is shown as a band of solid (dotted) lines for the W (Z).

The number of events in each p_T bin, ΔN, corrected for acceptance and resolution smearing, is used to derive the differential cross section as a function of p_T:

$$d\sigma/dp_T = \frac{\Delta N f_{DY}}{\Delta p_T \mathcal{L} B},$$

where $\mathcal{L} = 4.05 \pm 0.28$ pb^{-1} is the integrated luminosity [11], $f_{DY} = 0.987 \pm 0.005$ is the correction for the Drell-Yan continuum contribution to the Z peak, and $B = 0.033$ is the $Z \rightarrow ee(\mu\mu)$ branching ratio.

The results of the $d\sigma/dp_T$ measurement are summarized in Table I. The statistical fluctuations, as well as the systematic uncertainties in the corrections for resolution smearing, are correlated among the bins. To account for the correlation, we use a simple Monte Carlo procedure that models the results of a large number of experiments to obtain a covariance matrix. The uncorrelated variances, from the uncertainties on the normalization and the acceptance, are added to this covariance matrix to give the uncertainties and the correlation matrix presented in Table I.

The results are also shown in Fig. 2. The p_T values are corrected for binning effects such that, in the limit of infinite statistics, the plotted points lie on the true spectrum. The mean of the distribution is 11.5 ± 1.0 GeV/c. The results obtained separately for the $Z \rightarrow ee$ and $Z \rightarrow \mu\mu$ samples agree. The prediction of $d\sigma/dp_T$ from the QCD next-to-leading-order calculation is plotted as a band; the width of the band indicates the uncertainty in the prediction [1]. This prediction agrees with our result. We obtain a χ^2 of 5 for 13 degrees of freedom for the comparison between our result and the nominal QCD prediction (the median of the band in Fig. 2). For high-p_T Z production, we determine, for example, $\sigma(p_T > 50$ GeV/$c) = 135 \pm 51$ pb, or 2% of the integrated cross section. The QCD calculation predicts 154 ± 23 pb, in agreement with our measurement.

A comparison between the W and Z p_T spectra is shown in Fig. 3. A small difference is expected from QCD because of the different W and Z masses and the different couplings to the parton distributions as a function of p_T. But within the measurement uncertainties, the W and Z p_T spectra have the same shape.

We thank the Fermilab Accelerator Division staff and the CDF support staff for their dedicated effort that made this experiment possible. This work was supported by the Department of Energy, the National Science Foundation, Istituto Nazionale di Fisica Nucleare, the Ministry of Science, Education and Culture of Japan, and the A. P. Sloan Foundation.

[a] Visitor.
[1] P. B. Arnold and M. H. Reno, Nucl. Phys. **B319**, 37 (1989); P. B. Arnold and R. P. Kauffmann, Nucl. Phys. **B349**, 381 (1991).
[2] F. Abe *et al.*, Phys. Rev. Lett. **66**, 2951 (1991).
[3] C. Albajar *et al.*, Z. Phys. C **44**, 15 (1989); J. Alitti *et al.*, Z. Phys. C **47**, 523 (1990).
[4] F. Abe *et al.*, Nucl. Instrum. Methods Phys. Res., Sect. A **271**, 387 (1988).
[5] F. Abe *et al.*, Phys. Rev. D **44**, 29 (1991).
[6] F. Abe *et al.* (to be published).

[7] A high-p_T $Z \rightarrow ee$ candidate with $p_T = 210$ GeV/c and both electrons in the central region is observed in the raw data, but this event is not in the final data sample only because it comes from a bad-quality run with a number of channels not being read out in the plug EM calorimeter.

[8] F. Paige and S. D. Protopopescu, ISAJET Monte Carlo version 6.22, BNL Report No. BNL38034, 1986 (unpublished).

[9] A. D. Martin, R. G. Roberts, and W. J. Stirling, Phys. Rev. D **37**, 1161 (1988); M. Diemoz, F. Ferroni, E. Longo, and G. Martinelli, Z. Phys. C **39**, 21 (1988).

[10] J. S. T. Ng, Ph.D. thesis, Harvard University, 1991.

[11] The effective integrated luminosity for the muon sample is 3.54 ± 0.24 pb^{-1} because some runs are removed due to a muon trigger hardware problem. This is accounted for in the acceptance calculation.